Frontiers in Bioscience Landmark

Front. Biosci. (Landmark Ed) **2026**; 31(8): 52448
https://doi.org/10.31083/FBL52448

Original Research

Resveratrol Attenuates Gemcitabine Resistance in Hepatocellular Carcinoma Cells by Inhibiting Thymidylate Synthase

You Tang[1], Chuang Peng[1], Sulai Liu[1], Yunfeng Li[1], Siwei Zhu[1], Ya Zhu[2], Zhiguo Tan[3], Xu Chen[1,*], Ou Li[1,*]

[1]Department of Hepatobiliary Surgery, Hunan Provincial People's Hospital, The First Affiliated Hospital of Hunan Normal University, 410005 Changsha, Hunan, China
[2]Department of Hepatopancreatobiliary Surgery, The Second Affiliated Hospital of Kunming Medical University, 650000 Kunming, Yunnan, China
[3]The First School of Clinical Medicine, Lanzhou University, 730000 Lanzhou, Gansu, China
*Correspondence: chenxu941218@163.com (Xu Chen); leohnsry@iCloud.com (Ou Li)
Academic Editor: Amancio Carnero Moya
Submitted: 31 March 2026 Revised: 24 June 2026 Accepted: 3 July 2026 Published: 25 August 2026

Abstract

Background: Hepatocellular carcinoma (HCC) is a leading cause of cancer death worldwide. Gemcitabine (Gem) is a commonly used drug against HCC, but its efficacy is limited by the development of resistance. Resveratrol (Res), a natural polyphenol with antitumor activity, may reverse Gem resistance in HCC, although the mechanism remains unclear. **Methods:** The effects of Res on the proliferation, apoptosis, cell cycle, and invasion of Hep3B and HuH-7 cells were assessed via cell counting kit-8 (CCK-8), clonogenic, flow cytometry, and Transwell assays, respectively. Potential Res targets were predicted by network pharmacology, and markers of HCC prognosis were identified from the cancer genome atlas (TCGA) data. The interaction between Res and thymidylate synthase (TYMS) was validated by molecular docking and dynamics simulation. A Gem-resistant HuH-7 cell line (HuH-7/GR) was established, and when these cells were treated with Res combined with Gem, the effect on Gem sensitivity was detected by CCK-8 assay, clonogenic assay, and flow cytometry. Finally, a subcutaneous nude mouse model of HCC was used to evaluate the *in vivo* effects of Res combined with Gem. **Results:** Res inhibited HCC cell proliferation, induced apoptosis and G2/M arrest, and suppressed invasion in a concentration-dependent manner. Network pharmacology and TCGA analysis identified TYMS as an important target gene for Res. TYMS was highly expressed in HCC tissues and correlated with poor prognosis. Res treatment reduced TYMS expression, while molecular docking and simulation showed stable binding of Res to TYMS. TYMS levels were elevated in HuH-7/GR resistant cells. Res combined with Gem was found to reverse drug resistance, inhibit proliferation and colony formation, and induce apoptosis. The Res + Gem combination group showed the smallest tumor volume in the *in vivo* model. **Conclusion:** By attenuating Gem resistance through TYMS inhibition, Res holds promise as a clinically viable adjunct to Gem-based chemotherapy, offering a potential strategy to improve outcomes in HCC patients.

Keywords: hepatocellular carcinoma; resveratrol; drug resistance; gemcitabine; thymidylate synthase

1. Introduction

Hepatocellular carcinoma (HCC) is the leading histological subtype of primary liver neoplasms, with a global case proportion of 75%–85%. The incidence and mortality of HCC continue to increase worldwide [1,2]. Due to the occult onset of HCC, most patients are diagnosed in the middle and late stages of disease, which is too late for surgical resection. For these patients, systemic chemotherapy is the main treatment method [3,4]. Gemcitabine (Gem) is a nucleoside analog that interrupts DNA synthesis by incorporating into DNA strands. It is the basic chemotherapy drug for the treatment of a variety of solid tumors, including HCC [5]. However, the acquired resistance of tumor cells to Gem greatly limits its clinical efficacy, leading to chemotherapy failure and tumor recurrence [6]. Therefore, finding sensitizers that can safely and effectively reverse Gem resistance, and elucidating the molecular mechanism of resistance should help to improve the survival outcome of HCC patients.

Thymidylate synthase (TYMS) serves as a critical rate-limiting enzyme within the DNA biosynthetic pathway. It catalyzes the methylation of deoxyuridine (dUMP) to deoxythymidine (dTMP), providing an essential raw material for DNA replication and repair [7,8]. The activity of TYMS directly determines the supply of thymidine in cells, which in turn affects the rate of cell proliferation and genomic stability [9]. TYMS overexpression has been reported to be an important mechanism leading to tumor cell resistance to various anti-metabolic drugs, including Gem [10]. As a widely used anti-tumor nucleoside analog, Gem exerts its pharmacological effects mainly by inhibiting ribonucleotide reductase and interfering with DNA strand elongation [11]. However, abnormally high expression of TYMS can effectively maintain the balance of the intracellular deoxynucleotide triphosphate (dNTP) pool, especially by increasing the generation of deoxythymidine triphosphate (dTTP) to counteract depletion of the nucleotide pool. This weakens the effect of Gem-induced DNA damage

[12] and helps tumor cells maintain their DNA repair and synthesis abilities, thereby avoiding the lethal effects of chemotherapy drugs. TYMS level in HCC is generally significantly upregulated, in line with the highly proliferative nature of HCC [13]. TYMS overexpression in HCC tissues is related with the increasing tumor invasiveness, decreasing differentiation, and poor patient prognosis [14]. Thus, TYMS functions not merely as a critical regulator in liver cancer development and progression, but also holds promise as a prognostic biomarker and a therapeutic target for overcoming chemotherapy resistance.

Resveratrol (Res) is a natural polyphenolic compound found in plants such as grapes and Polygonum cuspidatum. It has attracted considerable attention due to its wide pharmacological activity, especially its anti-tumor properties [15,16,17]. It has been previously demonstrated that Res exerts anti-tumor effects by suppressing cell proliferation, triggering apoptosis, and potentiating chemosensitivity, which are mediated through the modulation of multiple signaling cascades, including the phosphoinositide 3-kinase (PI3K)/protein kinase B (Akt) signaling pathway (PI3K/Akt) and mitogen-activated protein kinase (MAPK) pathways [18,19]. Res has been reported to suppress HCC cell proliferation, migration, and invasion through modulation of the hypoxia-inducible factor-1α/vascular endothelial growth factor HIF-1α/VEGF signaling cascade [20]. Moreover, it was reported to reverse the resistance of HCC to cisplatin by inhibiting glutamine metabolism [21]. However, whether Res can reverse the resistance of HCC to Gem is currently unknown.

Therefore, the goal of this study was to explore the effect of Res on Gem resistance in HCC cells, as well as the potential molecular mechanisms involved. We integrated network pharmacology and the cancer genome atlas (TCGA) database analysis to identify Res targets and HCC-related genes. Furthermore, HCC cell lines and a subcutaneous HCC model in nude mice were employed to evaluate the effect of combined Res and Gem intervention, and to study the effect of Res on Gem resistance in HCC. Our results support a new theoretical basis to overcome chemotherapy resistance in HCC, as well as potential combination therapy strategies.

2. Materials and Methods

2.1 Cell Culture and Drug Treatment

Hep3B (#CL-0102) and HuH-7 (#CL-0120) cells, both derived from human hepatocellular carcinoma, were acquired from Wuhan ProCell Company (Wuhan, Hubei, China). Their cell origin was validated by short tandem repeat (STR), and the results of mycoplasma contamination testing were negative. Cells were incubated at 37 °C in a humidified 5% CO_2 atmosphere and cultured in Dulbecco's Modified Eagle Medium (DMEM) medium supplemented with 10% fetal bovine serum (FBS) and 1% penicillin-streptomycin. All experiments were performed using cells at passages 5 to 15 after thawing. The Gem resistant cell line HuH-7/GR was established by gradually increasing the concentration of Gem in the culture medium until the cells ultimately showed stable growth in a medium containing 50 nM Gem. Res and Gem were obtained from Sigma Aldrich (St. Louis, MO, USA), prepared as stock solutions in dimethyl sulfoxide (DMSO), and kept at –20 °C until further use.

2.2 Cell Counting Kit-8 (CCK-8) Assay

The CCK-8 assay kit (Dojindo Laboratories, Mashiki, Kumamoto, Japan) was employed to measure cell viability. Cells were inoculated into a 96-well plate with 5000 cell per well and treated with different concentrations various 0 to 120 μM of drugs for 24 h. Next, 10 μL of CCK-8 reagent was introduced into each well, followed by a 2-hour incubation period. The optical density at 450 nm was subsequently recorded using an enzyme-linked immunosorbent assay (ELISA) microplate reader (Thermo Fisher Scientific, Waltham, MA, USA).

2.3 Clone Formation Assay

After drug treatment, the cells were trypsinized and seeded into a 6-well plate at 800 cells/well where they were cultured for 14 days. The colonies were subsequently fixed using methanol, subjected to 0.1% crystal violet staining, and those harboring ≥50 cells were scored.

2.4 Analysis of Cell Apoptosis

Apoptosis was assessed using the Annexin V-fluorescein isothiocyanate (FITC)/propidium iodide (PI) dual staining kit (#SNK-007, Sunncell, Wuhan, China). Following 24 hours of drug treatment, the cells were harvested along with the supernatant. Annexin V-FITC and PI were applied as per the manufacturer's protocol. The cells were then incubated in the dark for 15 minutes, followed by analysis on a CytoFLEX Flow Cytometer (Beckman Coulter, Inc., Brea, CA, USA). Cells were first gated by FSC/SSC to remove debris, followed by FSC-A/FSC-H gating to exclude doublets. For apoptosis, quadrant gates were set using unstained and single-stained controls to define viable ($FITC^-/PI^-$), early apoptotic ($FITC^+/PI^-$), late apoptotic ($FITC^+/PI^+$), and necrotic ($FITC^-/PI^+$) populations.

2.5 Cell Cycle Analysis

Cell cycle distribution was assessed using the PI/RNase staining kit (#SNK-015, Sunncell, Wuhan, China). Following 24 hours of drug treatment, the cells were harvested and fixed overnight in 70% ethanol at 4 °C. Subsequently, PI/RNase staining solution was introduced, and the samples were incubated at 37 °C in the dark for 30 minutes. DNA content was quantified by flow cytometry, and cell cycle phase distribution was analyzed on a CytoFLEX Flow Cytometer (Beckman Coulter, Inc., Brea,

CA, USA). For cell cycle, singlet cells were analyzed for PI fluorescence (FL2-A), and sub-G1 debris was excluded.

2.6 Transwell Assay

The Transwell inserts (#3422; Corning, Corning, NY, USA) were pretreated by coating with Matrigel basement membrane matrix. The upper Transwell inserts received the cell suspension prepared in serum-free medium, whereas the lower compartment was replenished with growth medium supplemented with 10% FBS to function as a chemotactic gradient. At 24 hours post-seeding, cells that had not migrated through the membrane were carefully scraped off the upper chamber using a cotton swab. Cells that had migrated to the lower surface were subsequently fixed in methanol and subjected to crystal violet staining. Five random fields of view were then selected for cell counting under the microscope (Olympus CX23, Olympus Corporation, Tokyo, Japan).

2.7 Scratch Healing Assay

Cells were dispensed into 6-well plates and incubated until a confluent monolayer was formed. A 200 µL sterile pipette tip was then used to draw a line on the surface of the cell monolayer to create scratches. After washing with PBS to remove shed cells, maintenance medium containing 2% FBS was added for further cell culture. At 0 h and 24 h after scratching, photos were taken under an inverted microscope. The scratch area was measured using ImageJ software (National Institutes of Health, Bethesda, MD, USA).

2.8 Network Pharmacology and Bioinformatics Analysis

Potential targets were obtained from the PharmMapper (http://www.lilab-ecust.cn/pharmmapper/), SwissTarget Prediction (http://www.swisstargetprediction.ch/), and STITCH databases (http://stitch.embl.de). The Res target set was obtained after deduplication. HCC-related targets were obtained from GeneCards (http://www.genecards.org) using the keyword 'hepatocellular carcinoma' and the intersection of the two target sets was identified as potential Res targets against HCC. Data from the TCGA hepatocellular carcinoma (LIHC) project were utilized to examine the differential expression patterns of the overlapping genes in tumor versus normal tissues. To identify genes with prognostic significance, Kaplan-Meier survival analysis was conducted via the GEPIA2 web tool. Gene ontology (GO) and Kyoto encyclopedia of genes and genomes (KEGG) enrichment analyses of the *TYMS* gene were also performed.

2.9 Quantitative Real-Time Polymerase Chain Reaction (qRT-PCR)

RNA was isolated from cell pellets using TRIzol reagent (#15596026, Thermo Fisher Scientific, Waltham, MA, USA), after which the purified RNA was reverse-transcribed to cDNA. Quantitative polymerase chain reaction (qPCR) was performed using the SYBR Green method (#A25742, Thermo Fisher, Waltham, MA, USA) to determine TYMS mRNA levels, with β-actin used as an internal control. The primer sequences for TYMS were 5′-TACAGCCTGAGAGATGAATTCCC-3′ (forward) and 5′-GGATTCCAAGCGCACATGAT-3′ (reverse). Primer sequences for β-actin were 5′-ACATGGGGCAGTATGGCTTG-3′ (forward) and 5′-AGAGGTCACACTCGGGTTCA-3′ (reverse).

2.10 Western Blotting

Total cellular proteins were extracted with radioimmunoprecipitation assay (RIPA) lysis buffer (#P0013E-1; Beyotime, Shanghai, China) supplemented with protease inhibitor phenylmethylsulfonyl fluoride (PMSF) (#SH0906; Beyotime), and the resulting protein concentrations were assessed using the bicinchoninic acid (BCA) method. The extracted proteins were electrophoretically resolved using SDS-PAGE (#P0901M; Beyotime Biotechnology, Shanghai, China), followed by electrophoretic transfer to polyvinylidene difluoride (PVDF) membranes. Nonspecific binding was blocked by incubating the membrane in 5% non-fat dry milk, followed by overnight probing at 4 °C with rabbit anti-TYMS (#3766; Cell Signaling Technology; dilution 1:1000) and mouse anti-β-actin (#4967; Cell Signaling Technology; dilution 1:2000) primary antibodies. The next day, HRP-labeled secondary antibodies (anti-rabbit IgG, #7074, dilution 1:2000; anti-mouse IgG, #7076, dilution 1:2000, Cell Signaling Technology, Danvers, MA, USA) were incubated and an ECL chemiluminescence method (#32109, Thermo Fisher Scientific, Waltham, MA, USA) was used to detect protein grayscale.

2.11 Cell Transfection

Lipofectamine™ 3000 transfection reagent (#L3000015, Invitrogen, Carlsbad, CA, USA) was employed for siRNA delivery according to the manufacturer's specifications. The specific siRNA was sourced from Miaoling Bio (Wuhan, Hubei, China). The primer sequences for Si-Control were 5′-UUCUCCGAACGUGUCACGUTT-3′ (forward) and 5′-ACGUGACACGUUCGGAGAATT-3′ (reverse), and for Si-TYMS they were 5′-CAAUCCGCAUCCAACUAUUTT-3′ (forward) and 5′-AAUAGUUGGAUGCGGAUUGTT-3′ (reverse). Transfection efficiency was subsequently validated through qRT-PCR and Western blot analyses.

2.12 Molecular Docking and Molecular Dynamics Simulation

The three-dimensional coordinates of TYMS were acquired from the Protein Data Bank (PDB), while the structural information for Res was retrieved from the PubChem compound database. AutoDock Vina v1.1.2 (The Scripps Research Institute, La Jolla, CA, USA). was used to ana-

lyze molecular docking, and the conformation with the lowest binding energy was selected as the initial binding mode. The GROMACS software package was used for molecular dynamics simulation (simulation time set to 100 ns) and to analyze root mean square deviation (RMSD) and binding free energy.

2.13 Subcutaneous Tumors in Nude Mice

Four- to six-week-old male BALB/c nude mice (n = 20 in total) were obtained from Hunan SJA Laboratory Animal Co., Ltd. (Changsha, China). After a 7-day acclimatisation period, 5×10^6 HuH-7 cells were subcutaneously inoculated into the right axilla of each mouse. Based on the exploratory nature of the study and previous similar reports, no formal sample size calculation was performed, and 5 mice per group were used. No predefined inclusion/exclusion criteria were applied, and all animals were included in the analysis. Once tumours were established, mice were randomly assigned to four groups (n = 5 each) using a computer generated sequence by an independent researcher: Vehicle control, Gem (50 mg/kg, i.p., twice weekly), Res (50 mg/kg, gavage, daily), and Gem + Res combination. Treatment lasted 3 weeks. Doses and routes were chosen based on pilot experiments and published data. To minimise confounders, cage locations were rotated, treatment/measurement order was alternated across groups, and all measurements were performed by the same investigator. Blinding was applied during allocation, treatment, outcome assessment, and data analysis. At endpoint, mice were anesthetised with isoflurane (3–5% for induction, 1.5–2.5% for maintenance) and euthanised by cervical dislocation. Tumours were excised, weighed, and measured ($V = 0.5 \times \text{length} \times \text{width}^2$). Liver and kidney tissues were also collected for paraffin embedding and section staining. All animal procedures were approved by the Institutional Animal Committee of Hunan Provincial People's Hospital (No.2025-089).

2.14 Statistical Analysis

Each experiment was repeated at least three times, and all values are reported as the mean ± standard deviation (SD). Normality and homogeneity of variance were assessed using Shapiro-Wilk and Levene's tests, respectively; non parametric alternatives were applied when assumptions were violated. The IC50 value was calculated by nonlinear regression using SPSS 27.0 (IBM Corp., Chicago, IL, USA). Other statistical analyses were performed using GraphPad Prism 9.0 (San Diego, CA, USA). Differences between two groups were evaluated by the *t*-test, while one-way or two-way analysis of variance (ANOVA) was applied for comparisons involving three or more groups. The threshold for statistical significance was set at $p < 0.05$.

3 Results

3.1 Res Inhibits HCC Cell Proliferation and Invasion, and Induces Apoptosis and Cell Cycle Arrest

To investigate the effect of Res on HCC cells, we first treated Hep3B and HuH-7 cells with different concentrations of Res (0, 10, 20, 40, 80, and 120 μM). The CCK-8 results showed that Res significantly inhibited the viability of both cell lines in a concentration-dependent manner, with IC_{20} values of 9.53 ± 2.14 μM for Hep3B and 9.87 ± 1.96 μM for HuH-7 (Fig. 1A). Based on this, we chose 10 μM as the treatment concentration for subsequent experiments. As shown in Fig. 1B, treatment with 10 μM Res significantly inhibited the colony-forming capacity of Hep3B and HuH-7 cells ($p < 0.01$). The flow cytometry results showed that rates of early and late apoptosis in the Res treatment group were significantly higher than those in the control group ($p < 0.01$) (Fig. 1C). Cell cycle analysis showed that Res treatment led to a significant increase in the proportion of G2/M phase cells, whereas G0/G1 phase cells decreased, indicating that cells were blocked in the G2/M phase (Fig. 1D). In addition, the scratch healing assay and the Transwell assay showed that Res could effectively inhibit the invasion and migration ability of HCC cells (Fig. 1E,F).

3.2 Network Pharmacology Prediction of Potential Res Targets With Anti-HCC Effects

The structure of Res is shown in Fig. 2A. By integrating multiple databases, a total of 100 Res-related targets were obtained. The top 500 HCC-related targets were retrieved from the GeneCards database (**Supplementary Table 1** and **Supplementary Table 2**). After intersecting the two target sets, 24 common potential targets were obtained (Fig. 2B,C). These 24 genes were considered candidate target genes through which Res may exert anti-HCC effects, and their expression in HCC was analyzed using data from the TCGA database. Amongst them, 12 genes were highly expressed in HCC, including *TYMS*, TNF receptor-associated factor 1 (*TRAF1*), and mammalian target of rapamycin (*MTOR*). The remaining 12 genes showed either decreased expression in HCC, or did not show significant changes compared to normal liver tissue (Fig. 2D, **Supplementary Fig. 1**).

3.3 TYMS is a Key Target and is Associated With the Prognosis of HCC

Next, we further analyzed the 12 candidate target genes that were highly expressed in HCC. We examined their expression levels in HCC and their association with patient prognosis, including overall survival (OS), disease-specific survival (DSS), and progression-free interval (PFI). TYMS was found to be the only gene in which high expression was significantly associated with all the OS, DSS and PFI of HCC patients. Specifically, patients with high expression of TYMS had significantly shorter OS (HR = 1.67, $p = 0.004$), DSS (HR = 2.21, $p < 0.001$), and PFI (HR

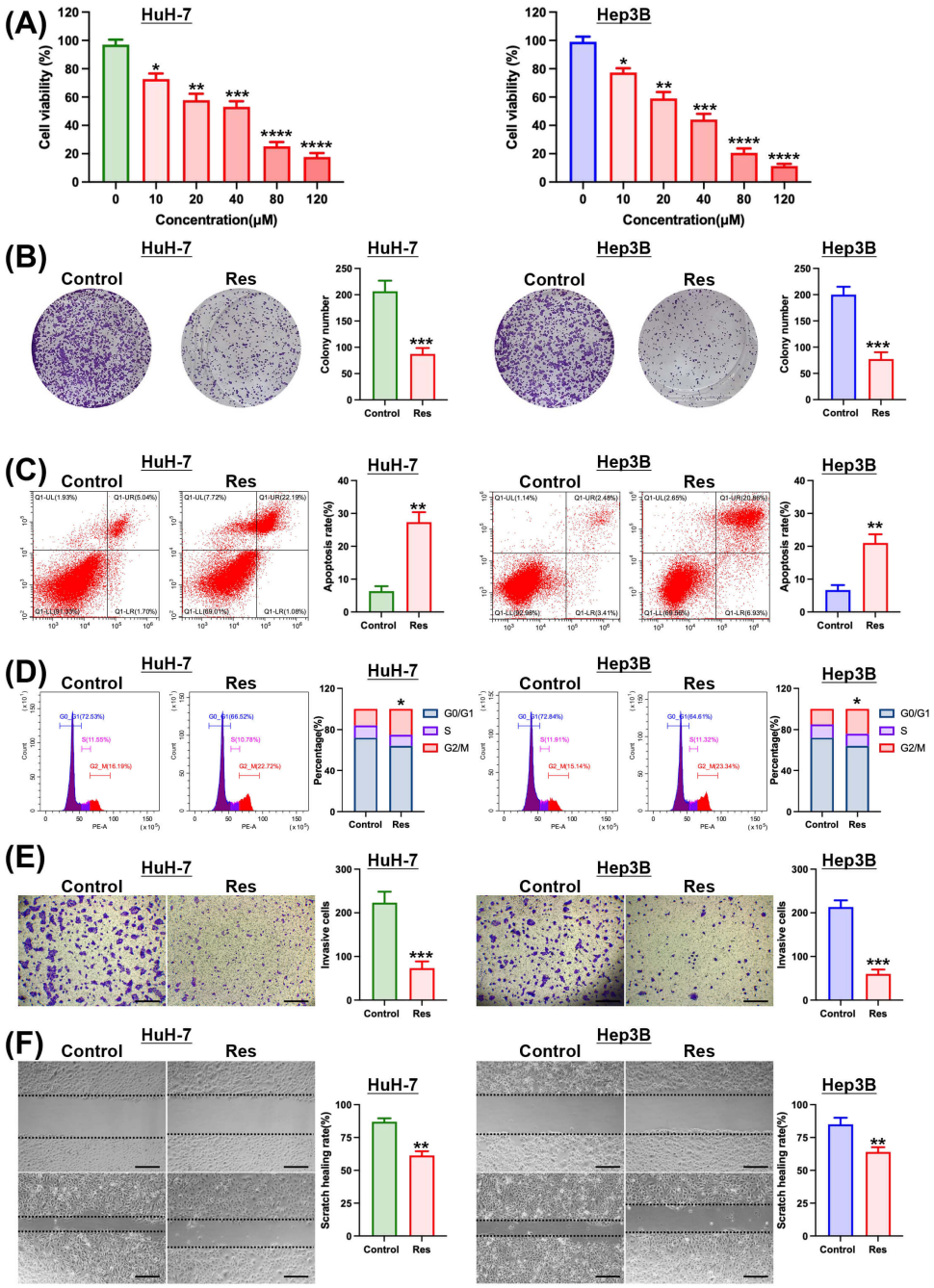

Fig. 1. Res inhibited HCC cell proliferation and invasion, and induced apoptosis and cell cycle arrest. (A) The CCK-8 assay was performed to detect cell viability in HuH-7 and Hep3B cells treated with different concentrations of Res (0, 10, 20, 40, 80, and 120 μM) for 24 h. (B) A clonogenic formation assay was used to evaluate the colony-forming ability of HuH-7 and Hep3B cells after Res (10 μM) treatment. (C) Flow cytometry analysis was conducted to measure the apoptosis rate of HuH-7 and Hep3B cells following Res (10 μM) treatment. The total apoptosis rate was calculated by Q1 UR + Q1 LR. The left panel was representative image and the bar graph showed the means of apoptosis rate. (D) The cell cycle distribution of HuH-7 and Hep3B cells treated with Res (10 μM) was analyzed by flow cytometry. (E) The Transwell invasion assay was employed to assess the invasive capacity of HuH-7 and Hep3B cells after Res (10 μM) treatment (scale bar = 200 μm). (F) Scratch healing assay was performed to determine the migration ability of HuH-7 and Hep3B cells treated with Res (10 μM) treatment (scale bar = 200 μm). Data are presented as the mean ± SD (n = 3). *$p < 0.05$, **$p < 0.01$, ***$p < 0.001$, ****$p < 0.0001$ vs. control group. HCC, Hepatocellular carcinoma; CCK-8, cell counting kit-8; Res, Resveratrol; SD, standard deviation.

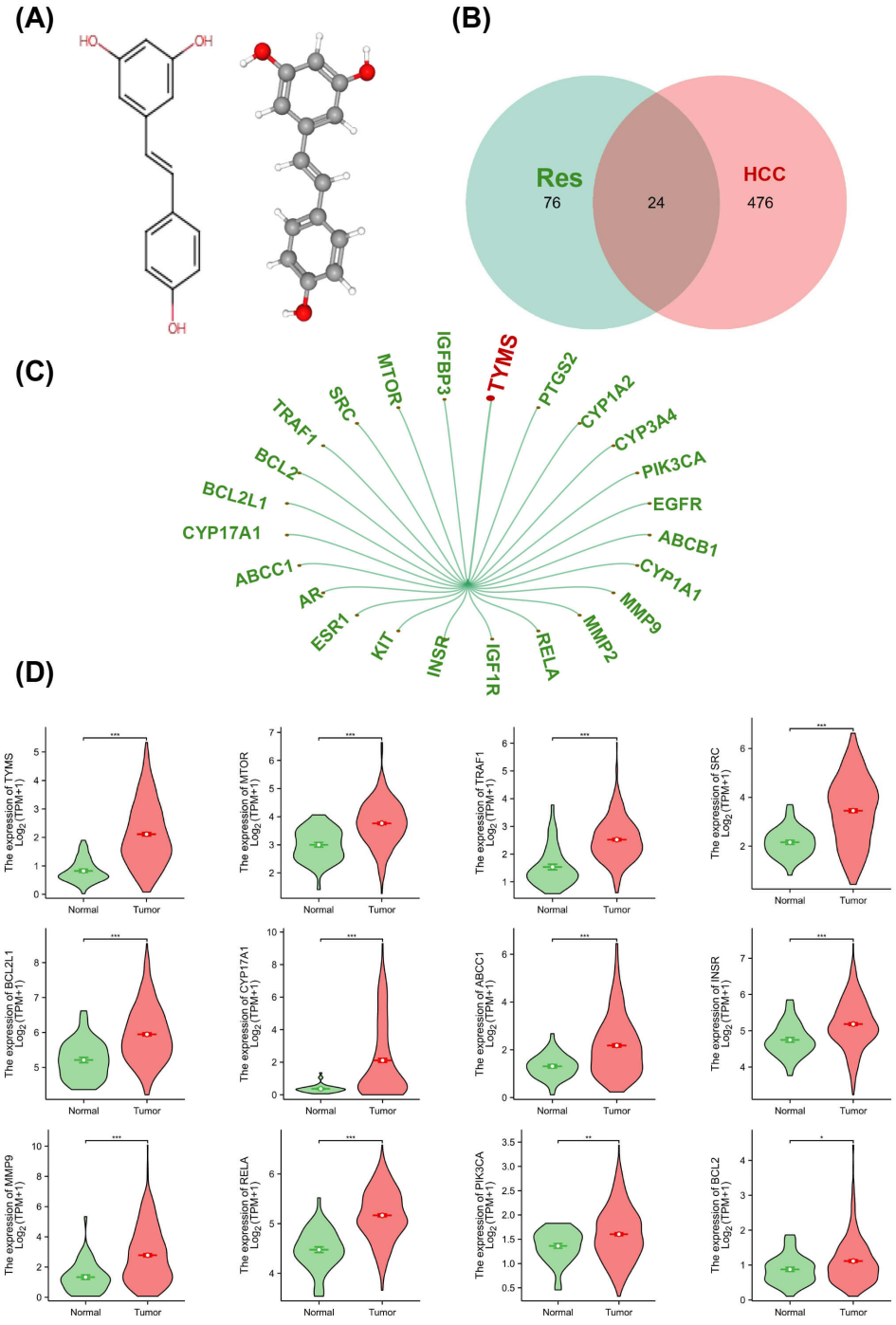

Fig. 2. Network pharmacology prediction of potential Res targets with anti-HCC effects. (A) Chemical structure and 3D molecular model of Res. (B) Venn diagram showing the overlap between Res-related target genes (n = 100) and HCC-related genes (n = 500), with 24 genes identified in the intersection. (C) The 24 intersection genes, with TYMS highlighted as a key hub gene. (D) Violin plots displaying the differential expression of 12 key target genes (*TYMS*, *MTOR*, *TRAF1*, *SRC*, *BCL2L1*, *CYP17A1*, *ABCC1*, *INSR*, *MMP9*, *RELA*, *PIK3CA*, *BCL2*) between normal liver tissues and HCC tumor tissues (***$p < 0.001$, **$p < 0.01$, *$p < 0.05$).

= 1.68, $p < 0.001$) compared to patients with low expression of TYMS (Fig. 3A–C, **Supplementary Fig. 2**). GO and KEGG enrichment analyses suggested that TYMS was mainly involved in pathways involving DNA replication, cell cycle, etc. (Fig. 3D–K).

3.4 Res May Bind Directly to TYMS and Reduce its Expression

Considering the stable drug-metabolizing enzyme activity of HuH-7 cells [22], we conducted further mechanistic studies with these cells in subsequent experiments.

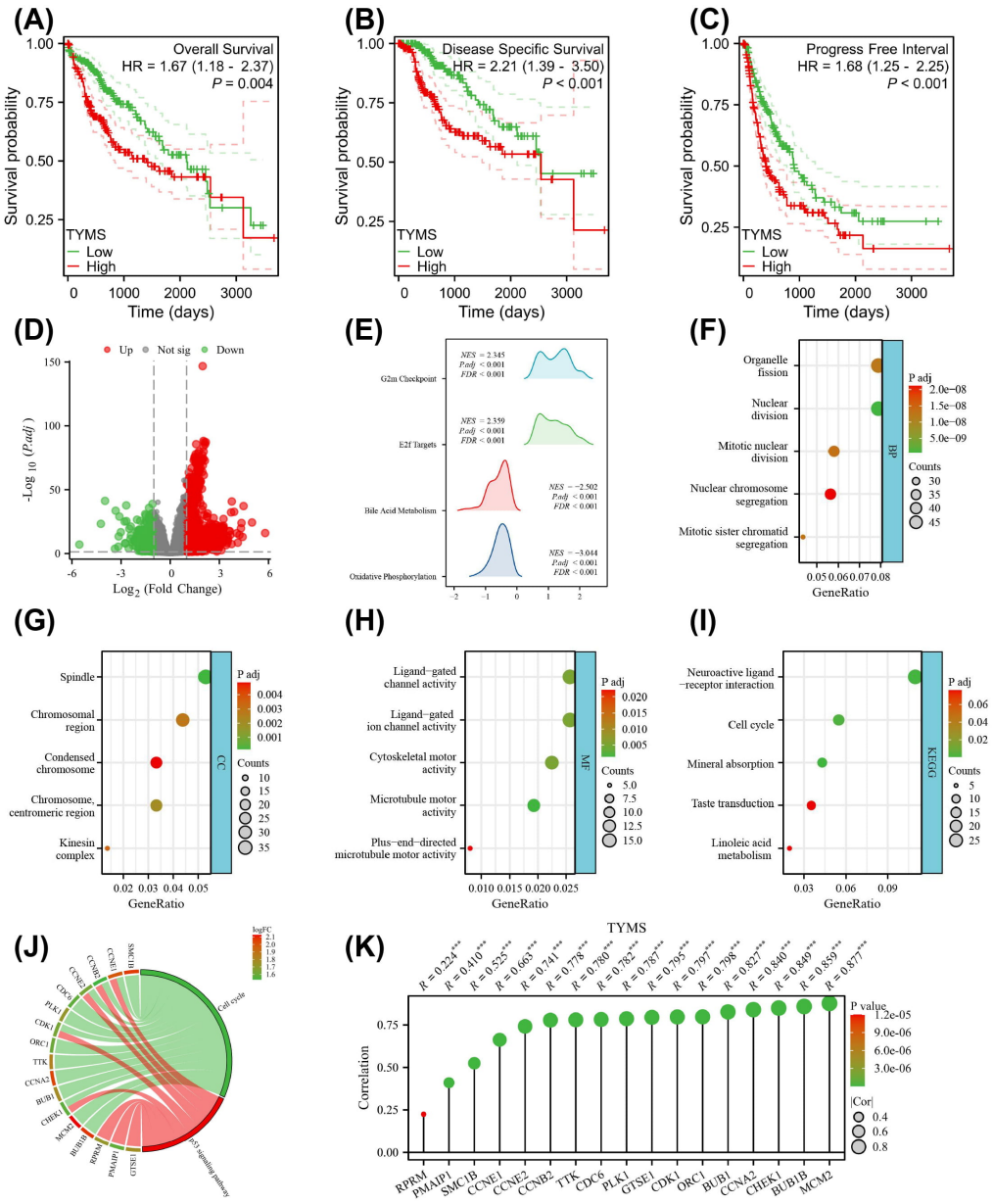

Fig. 3. TYMS is a key target gene, and its expression is associated with the prognosis of HCC. (A) Kaplan–Meier survival curves showing overall survival (OS) in HCC patient groups with different TYMS expression levels. (B) Kaplan–Meier survival curves showing disease-specific survival (DSS) in HCC patient groups with different TYMS expression levels. (C) Kaplan–Meier survival curves showing progression-free interval (PFI) in HCC patient groups with different TYMS expression levels. (D) Volcano plot of differentially expressed genes (DEGs) between TYMS-high and TYMS-low HCC subgroups (red: upregulated; green: downregulated; gray: not significant). (E) Gene set enrichment analysis (GSEA) revealed the top-enriched pathways in TYMS-high HCC, including G2M Checkpoint, E2F Targets, Bile Acid Metabolism, and Oxidative Phosphorylation. (F) Biological Process (BP) terms enrichment analyses of DEGs. (G) Cellular Component (CC) terms enrichment analyses of DEGs. (H) Molecular Function (MF) terms enrichment analyses of DEGs. (I) KEGG pathways enrichment analyses of DEGs. (J) Circular plot showing co-expression correlations between TYMS and cell cycle-related genes. (K) Correlation lollipop demonstrating strong positive correlations between TYMS and key cell cycle genes. ***$p < 0.001$.

TYMS expression changes were detected in HuH-7 cells after Res treatment. After 24 h treatment of HuH-7 cells with 10 μM Res, the TYMS mRNA and protein levels decreased significantly (Fig. 4A). The molecular docking results showed that Res can stably bind to the active pocket of the TYMS protein, with a binding energy of –7.1 kcal/mol (Fig. 4B). Further molecular dynamics simulations (100 ns) showed that the RMSD value of the Res TYMS complex

remained stable during the simulation, indicating a stable binding conformation (Fig. 4C–H). We speculate that binding of Res to TYMS may inhibit its enzymatic activity.

3.5 Res Reverses the Resistance of HuH-7 Cells to Gem

Given that TYMS is closely linked to the cell cycle, we further investigated its effect on cell resistance to Gem. We first constructed a Gem-resistant cell line, HuH-7/GR. The IC_{50} value of Gem in HuH-7/GR cells (533.56 ± 6.72 nM) was found to be 4–fold higher than that of parental HuH-7 cells (132.08 ± 3.65 nM) (**Supplementary Table 3**). Moreover, the TYMS protein level in HuH-7/GR cells was significantly upregulated compared to HuH-7 cells (Fig. 5A).

Next, we successfully constructed HuH-7/GR cells with TYMS knockdown. The mRNA and protein levels of TYMS in the si-TYMS group were confirmed to be significantly lower than those in the control group (**Supplementary Fig. 3A**). Furthermore, the IC_{50} value of Gem in si-TYMS cells (220.64 ± 13.37 nM) was lower than that of HuH-7/GR cells (**Supplementary Table 4**). Therefore, knockdown of TYMS caused HuH-7/GR cells to be more sensitive to Gem, and the combination of Res+Gem significantly inhibited cell proliferation (**Supplementary Fig. 3B**). Subsequently, we examined the sensitizing effect of Res on drug-resistant cells. In HuH-7/GR cells, the combination of Res (10 μM) and Gem significantly reduced cell viability and colony formation ability compared to the use of Gem alone, and significantly increased the cell apoptosis rate (Fig. 5B–F). These results indicate that Res could effectively restore the sensitivity of HuH-7/GR cells to Gem.

3.6 Res Combined With Gemcitabine Inhibits Tumor Growth In Vivo

HuH-7 cells were also utilized to construct a subcutaneous tumor model in nude mice. Both the Res and Gem monotherapy groups showed inhibition of tumor growth compared to the control group, but the effect was limited (Fig. 6A). The tumor volume and weight of the combination therapy group (Res+Gem) were significantly smaller than those of the other three groups. The results of ALT, AST, UA, UREA, and H&E staining of liver and kidney showed that the various treatments were safe and did not damage liver and kidney functions (Fig. 6B,C). The H&E staining and PCNA staining of tumor tissues revealed that the combination group had the lowest positivity rate for PCNA (Fig. 6D). In summary, the above results indicate that the combination of Res and Gem can effectively inhibit tumor growth *in vivo* without causing damage to liver and kidney functions.

4. Discussion

Resistance to Gem is an important obstacle in the treatment of advanced HCC, and overcoming this resistance is crucial to improving patient survival rates. This study revealed a novel mechanism by which Res reverses Gem resistance in HCC through its inhibition of TYMS. Our comprehensive analysis involving network pharmacology prediction, molecular biology validation, and *in vitro* and *in vivo* functional experiments confirmed the synergistic antitumor effect of Res combined with Gem.

We initially verified that Res exerts inhibitory effects on HCC cell proliferation and migration, while also promoting apoptosis and inducing G2/M phase cell cycle arrest. Subsequently, we used network pharmacology methods to identify TYMS as a key molecule in the intersection between Res and HCC. TYMS is overexpressed in various tumor types and is the main target of antimetabolite drugs such as 5-fluorouracil and Gem. High expression levels of TYMS are associated with decreased drug efficacy [10,23]. TYMS overexpression in HCC was significantly linked to worse prognosis across OS, DSS, and PFI, highlighting its candidacy as a therapeutic target.

The present study also found that Res significantly downregulated the expression of TYMS. The results of the molecular dynamics simulation showed that Res could stably bind to the active site of TYMS, suggesting that it may act as a direct inhibitor of this enzyme. We observed a significant increase in TYMS level in the successfully constructed Gem-resistant cell line HuH-7/GR. Res treatment may effectively reduce the TYMS level in HuH-7/GR cells, thereby restoring their sensitivity to Gem. Although most studies suggest that inhibition of TYMS is associated with cell cycle arrest in the S phase, some studies have also suggested that TYMS inhibition is related to G2/M phase arrest in HCC. A previous study found that Res acts mainly in the G2/M phase in HCC, which is consistent with the current results [24,25,26].

The mechanism by which Res reverses drug resistance is likely to rely on its downregulation of TYMS, allowing Gem to exert its cytotoxic effects. TYMS is generally highly expressed in HCC tissues and cells, and this high expression is closely associated with poor patient prognosis [27]. TYMS primarily catalyzes the conversion of dUMP to dTMP, thus providing essential material for DNA repair and replication, and promoting the malignant proliferation and invasion of HCC cells [14,28]. Previous studies have shown that TYMS is an important target of the classic chemotherapy drug 5-fluorouracil (5-FU) [29]. However, the high expression of TYMS is one of the main reasons for the development of resistance to 5-FU in liver cancer cells. Therefore, a key factor in reversing drug resistance and improving the efficacy of chemotherapy is the effective inhibition of TYMS activity. Certain bioactive compounds derived from traditional Chinese medicine, including Huachansu toxin, have been shown to markedly suppress HCC cell proliferation and elicit DNA damage. The proposed mechanism is the promotion of proteasome-dependent degradation of the TYMS protein, thus reducing its cellular level [25,30]. The expression of TYMS is regulated by the transcription factor FOXM1, and FOXM1-

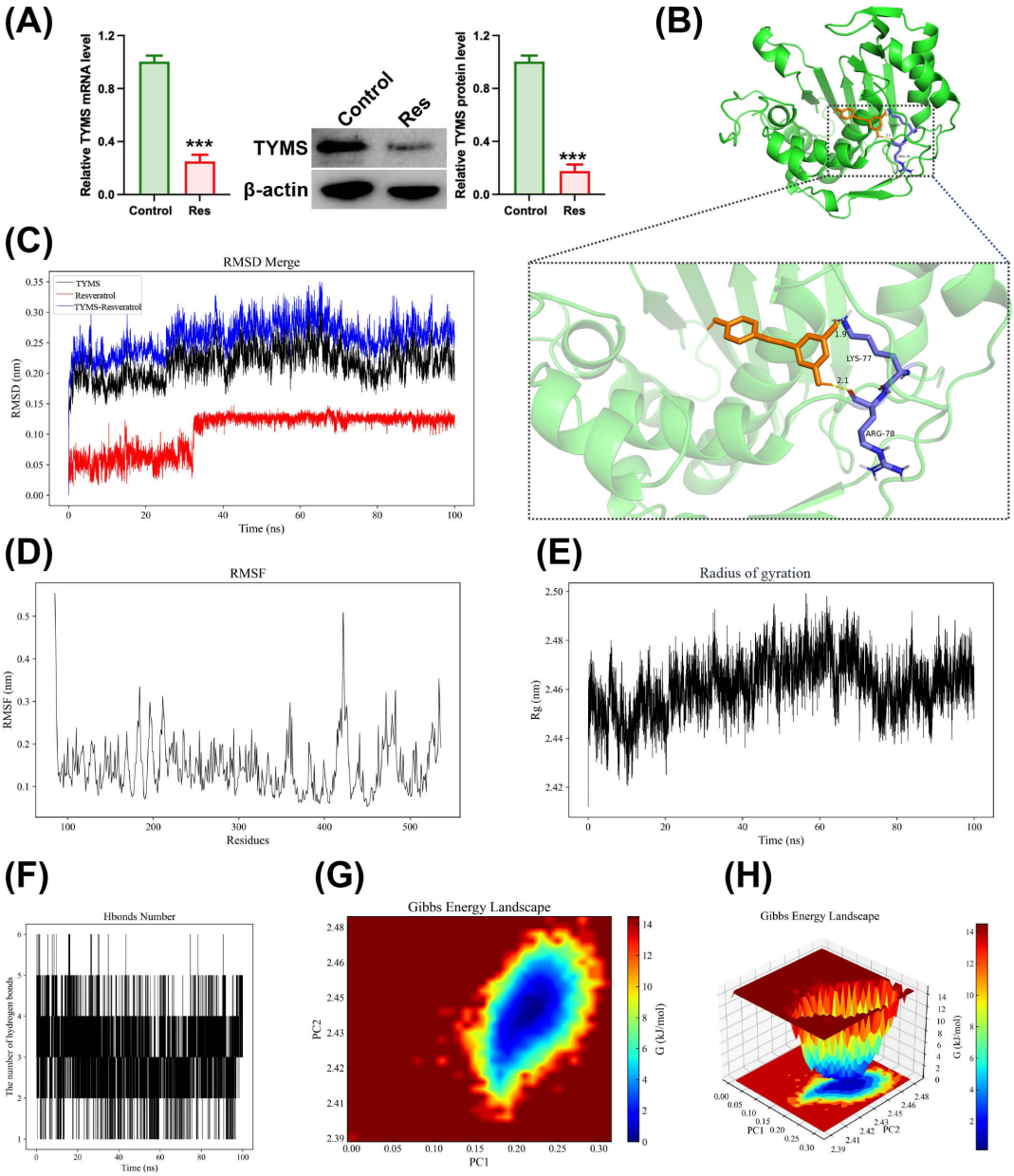

Fig. 4. Res may directly bind to TYMS and reduce its expression. (A) qRT-PCR and Western blot analyses showing that Res treatment significantly downregulated TYMS mRNA and protein levels in HCC cells. (B) 3D structural model of the TYMS–Res complex, with a detailed view of the binding pocket and key interacting residues (LYS77, ARG78). (C) Root Mean Square Deviation (RMSD) plot of TYMS (black), Res (red), and the TYMS–Res complex (blue) over a 100 ns molecular dynamics (MD) simulation, indicating system stability. (D) Root Mean Square Fluctuation (RMSF) plot of TYMS residues in a complex with Res, reflecting local protein flexibility. (E) Radius of gyration (Rg) plot of the TYMS–Res complex, demonstrating consistent protein compactness during the simulation. (F) Time-dependent number of hydrogen bonds between TYMS and Res, confirming stable intermolecular interactions. (G) 2D Gibbs energy landscape of the TYMS–Res complex along principal components PC1 and PC2, revealing a stable conformational cluster. (H) 3D Gibbs energy landscape corresponding to (G), visualizing the energy minimum of the TYMS–Res complex. ***$p < 0.001$ vs. control group. qRT-PCR, quantitative real-time polymerase chain reaction.

induced upregulation of TYMS is an important mechanism that promotes liver cancer progression and leads to 5-FU resistance [27]. Furthermore, TYMS is applied in combination with inhibitors of other metabolic enzymes, including ACLY and G6PD, and supplemented with retinoic acid for HCC treatment. This combination is designed to simultaneously block the synthesis of essential substances and the self-renewal ability of liver cancer cells through multiple pathways. In preclinical models, this combination has been demonstrated to have tumor suppressive effects beyond the

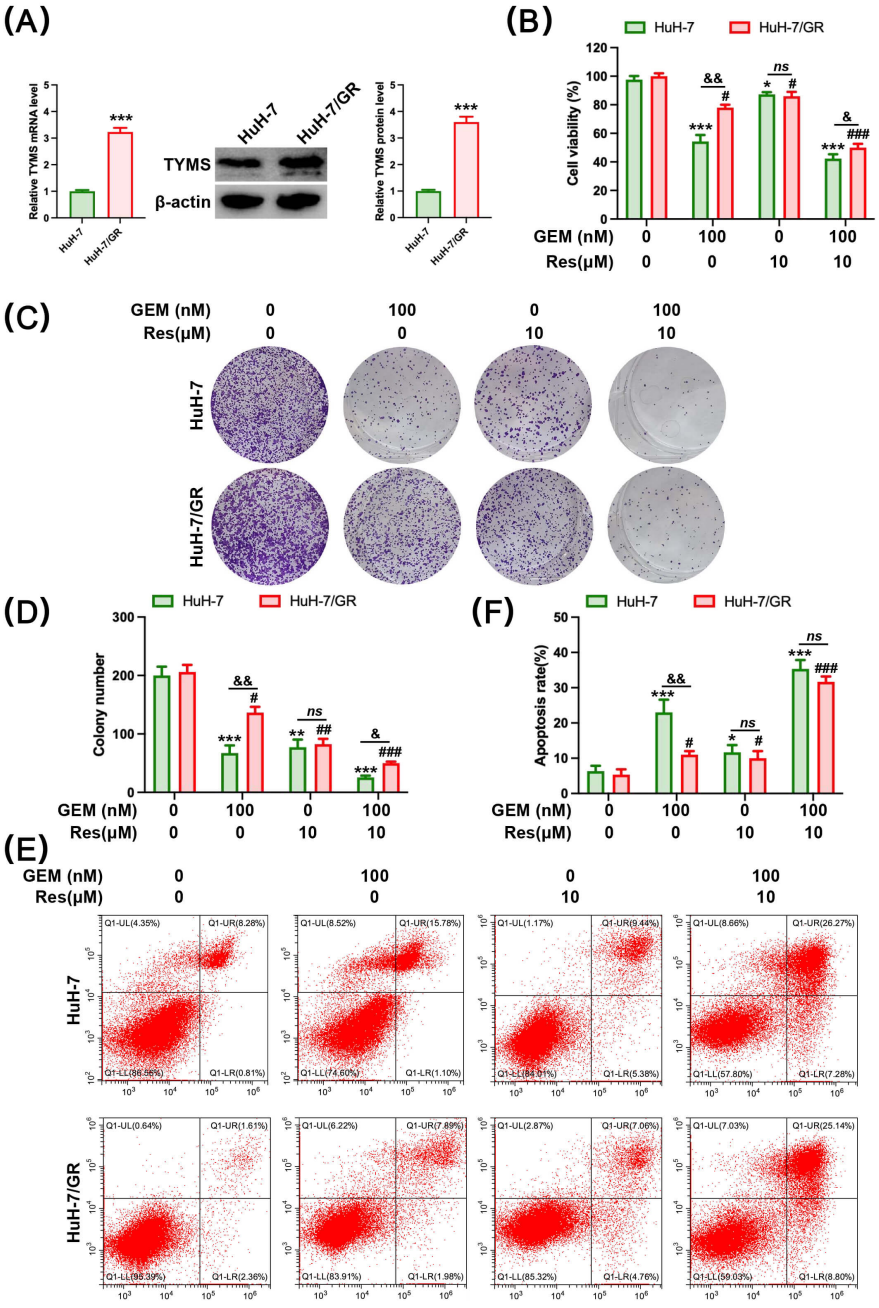

Fig. 5. Res reverses the resistance of HuH-7 cells to Gem. (A) qRT-PCR and Western blot analyses showing elevated TYMS mRNA and protein expression in HuH-7/GR (Gem-resistant HuH-7) cells compared with parental HuH-7 cells (***$p < 0.001$). (B) CCK-8 assay showing cell viability in HuH-7 and HuH-7/GR cells treated with GEM (100 nM), Res (10 μM), or their combination. (C,D) Clonogenic formation assay in HuH-7 and HuH-7/GR cells under the indicated treatments. (E,F) Flow cytometry showing apoptosis in HuH-7 and HuH-7/GR cells treated with GEM, Res, or their combination. *$p < 0.05$, **$p < 0.01$, ***$p < 0.001$ vs. HuH-7 control. $^{\#}p < 0.05$, $^{\#\#}p < 0.01$, $^{\#\#\#}p < 0.001$ vs. HuH-7/GR control. $^{\&}p < 0.05$, $^{\&\&}p < 0.01$ HuH-7/GR vs. HuH-7. ns $p > 0.05$. qRT-PCR, quantitative real-time polymerase chain reaction.

existing targeted drug sorafenib [31]. Therefore, targeting TYMS represents a promising therapeutic approach for HCC, and the ability of Res to suppress TYMS expression further supports its potential as an effective anti-HCC agent.

Being a natural compound, Res has demonstrated good safety and tolerability in clinical use for patients with knee osteoarthritis [32,33]. In the present study, *in vivo* experiments not only validated the significant anti-tumor effects of Res combined with Gem, but also demonstrated

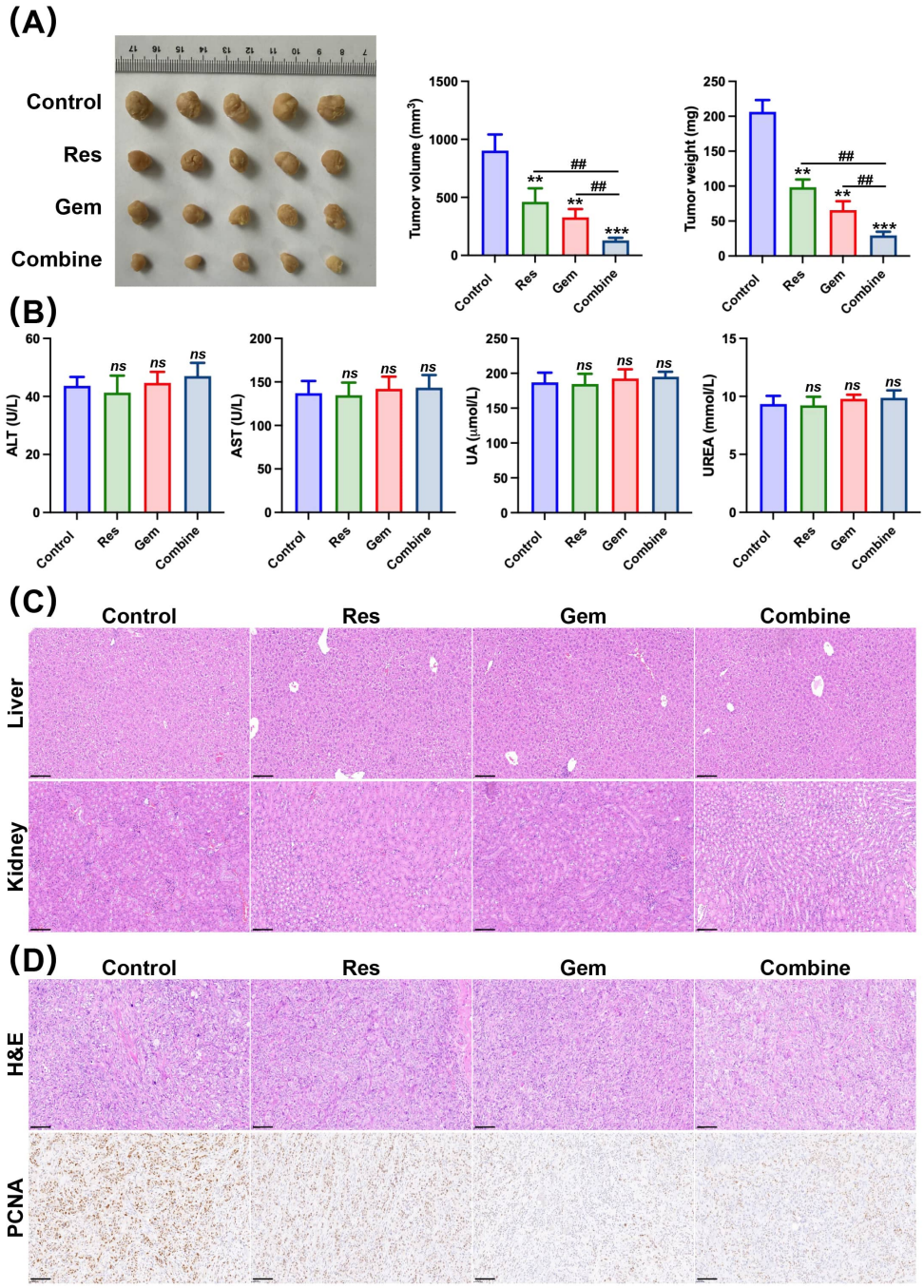

Fig. 6. Res combined with Gem inhibits tumor growth *in vivo*. (A) Representative images of xenograft tumors and quantitative analyses of tumor volume and weight in mice treated with Control, Res (50 mg/kg), Gem (50 mg/kg), or their combination (Combined). $^{**}p < 0.01$, $^{***}p < 0.001$ vs. Control group; $^{\#\#}p < 0.01$ vs. Combined group. (B) Serum biochemistry analyses of liver (ALT, AST) and kidney (UA, UREA) function markers in mice from each treatment group showed no significant differences (ns, $p > 0.05$) between groups, indicating minimal organ toxicity. (C) H&E staining of liver and kidney tissues from each treatment group (scale bar = 100 μm), confirming no obvious pathological damage in major organs. (D) Histological analyses of xenograft tumors: H&E staining and IHC for PCNA (scale bar = 100 μm). ALT, alanine aminotransferase; AST, aspartate aminotransferase; UA, uric acid; H&E, hematoxylin and eosin; IHC, Immunohistochemistry; PCNA, proliferating cell nuclear antigen.

preliminary safety. This work provides strong preclinical evidence for the future development of Res combined with Gem as adjuvant therapy for HCC patients with drug-resistant tumors.

5. Limitations

Although this study provides several novel insights, it has several limitations. First, the specific molecular mech-

anism by which Res downregulates TYMS, whether at the transcriptional or post-translational modification level, requires further clarification. Second, whether Res exerts its effect by affecting the metabolism of substrates (such as dUMP) or products (dTMP) of TYMS warrants further investigation through metabolomics.

6. Conclusion

In summary, this study found that TYMS is a key molecule mediating Gem resistance in hepatocellular carcinoma, and an important target of Res. Res can effectively reverse the resistance of HCC cells to Gem by binding to and inhibiting TYMS. Res combined with Gem showed significant and synergistic anti-tumor effects, both *in vitro* and *in vivo*. This study proposes a new target to overcome chemotherapy resistance in HCC, and suggests that Res may be useful as an adjuvant therapy for Gem in clinical practice.

Availability of Data and Materials

The datasets used and analyzed during the current study are available from the corresponding authors on reasonable request.

Author Contributions

OL, XC, and YT performed the experiment; OL and XC contributed significantly to analysis and manuscript preparation; YT, CP, SL, YL, SZ, YZ, ZT performed the data analyzes and wrote the manuscript; OL and XC contributed to the conception of the study. All authors contributed to editorial changes in the manuscript. All authors read and approved the final manuscript. All authors have participated sufficiently in the work and agreed to be accountable for all aspects of the work.

Ethics Approval and Consent to Participate

The use and care of the mice for this study were reviewed and approved by the Institutional Animal Committee of Hunan Provincial People's Hospital (the first affiliated hospital of Hunan Normal University) (No.2025-089). The animal experiments in the study were in compliance with the revised Animals (Scientific Procedures) Act 1986 in the UK and Directive 2010/63/EU in Europe. The ARRIVE guidelines 2.0 have been followed throughout this study.

Acknowledgment

Thanks to all the peer reviewers for their opinions and suggestions.

Funding

This work was financially supported by Hunan Provincial Natural Science Foundation (NO. 2025JJ80711), Leading talent project of Hunan Provincial People's Hospital (NO. 20230327-1012) and Scientific and Technological Innovation Team Project of Hunan Provincial People's Hospital (No. KCTG202502).

Conflicts of Interest

The authors declare no conflicts of interest.

Declaration of AI and AI-Assisted Technologies in the Writing Process

We acknowledge the use of Gemini 2 (Google) for assistance in generating the graphical abstract. The generated content was reviewed, edited, and revised by the authors as necessary. The authors take full and final responsibility for all content of this manuscript, including the accuracy, originality, and integrity of the information presented

Supplementary Material

Supplementary material associated with this article can be found, in the online version, at https://doi.org/10.31083/FBL52448.

References

[1] Aparicio B, Silva L, Ruiz M, Llópiz D, Repáraz D, Theunissen P, et al. Immunogenicity of neoantigens from hepatocellular carcinoma patients treated with a combined radioimmunotherapy. Oncoimmunology. 2026; 15: 2645280. https://doi.org/10.1080/2162402X.2026.2645280

[2] Gkatzionis A, Sanderson E, Smith GD, Stender S, Gellert-Kristensen H. Disentangling the Effect of BMI on Hepatocellular Carcinoma From Cirrhosis With Multivariable Mendelian Randomization. Liver International : Official Journal of the International Association for the Study of the Liver. 2026; 46: e70609. https://doi.org/10.1111/liv.70609

[3] Lei YR, He XL, Li K, Mo S. Drug resistance in hepatocellular carcinoma: theoretical basis and therapeutic aspects. Frontiers in Bioscience (Landmark Edition). 2024; 29: 52. https://doi.org/10.31083/j.fbl2902052

[4] Wu Y, Ju G, Zhou X, Wu J, Zheng S, Peng C. Targeting *WTAP* sensitizes hepatocellular carcinoma to sorafenib by inhibiting the ERK signaling pathway. Journal of Zhejiang University. Science. B. 2026; 27: 310–320. https://doi.org/10.1631/jzus.B2500191

[5] Louafi S, Boige V, Ducreux M, Bonyhay L, Mansourbakht T, de Baere T, et al. Gemcitabine plus oxaliplatin (GEMOX) in patients with advanced hepatocellular carcinoma (HCC): results of a phase II study. Cancer. 2007; 109: 1384–1390. https://doi.org/10.1002/cncr.22532

[6] Li N, Hu B, Liu C, Du K, Guo B, Yan M, et al. Targeting FUT1-mediated EGFR fucosylation and COX-2 reverses gemcitabine resistance by activating immunogenic cell death in hepatocellular carcinoma. Bioorganic Chemistry. 2025; 166: 109111. https://doi.org/10.1016/j.bioorg.2025.109111

[7] Sayed AE, Gomes N, Zakrzewski M, Liudkovska V, Serwa R, Azzi A. The mTORC2 component SIN1 post-transcriptionally regulates TYMS levels and modulates P53 activity in response to 5-FU chemotherapy. Cell Communication and Signaling : CCS. 2026; 24: 111. https://doi.org/10.1186/s12964-025-02640-y

[8] Vijayakurup V, Meyer B, Rizvi SR, Kievit KH, Hyder I, Koh J, et al. Integrated proteomic analysis identifies TYMS-dependent AMPK-mTOR signaling in pancreatic neuroendocrine tumors.

iscience. 2025; 28: 113833. https://doi.org/10.1016/j.isci.2025.113833

[9] Zhang X, Shi L, Gao Y, Zhou C, Wang X, Shi X. Chidamide enhances the sensitivity of gastric cancer to 5-fluorouracil chemotherapy by suppressing the HDAC3/HNF4A/TYMS axis. Cell Death & Disease. 2025; 17: 2. https://doi.org/10.1038/s41419-025-08247-y

[10] Weekes CD, Nallapareddy S, Rudek MA, Norris-Kirby A, Laheru D, Jimeno A, et al. Thymidylate synthase (TYMS) enhancer region genotype-directed phase II trial of oral capecitabine for 2nd line treatment of advanced pancreatic cancer. Investigational New Drugs. 2011; 29: 1057–1065. https://doi.org/10.1007/s10637-010-9413-7

[11] Chu CS, Chen HP, Lin PH, Cheng CC, Kuo HY, Fan PH, et al. Interleukin-1 receptor 1 deficiency worsens hepatocellular carcinoma, while gemcitabine treatment alleviates the hepatocellular carcinoma-induced increase in intra-hepatic immune cells. Journal of Gastroenterology and Hepatology. 2024; 39: 2208–2218. https://doi.org/10.1111/jgh.16674

[12] Dorman SN, Baranova K, Knoll JHM, Urquhart BL, Mariani G, Carcangiu ML, et al. Genomic signatures for paclitaxel and gemcitabine resistance in breast cancer derived by machine learning. Molecular Oncology. 2016; 10: 85–100. https://doi.org/10.1016/j.molonc.2015.07.006

[13] Li S, Zhao J, Lv L, Dong D. Identification and Validation of TYMS as a Potential Biomarker for Risk of Metastasis Development in Hepatocellular Carcinoma. Frontiers in Oncology. 2021; 11: 762821. https://doi.org/10.3389/fonc.2021.762821

[14] Abdel Allah HMM, Zahran WE, El-Masry SA, El-Bendary M, Soliman AF. Association of MTHFR and TYMS gene polymorphisms with the susceptibility to HCC in Egyptian HCV cirrhotic patients. Clinical and Experimental Medicine. 2022; 22: 257–267. https://doi.org/10.1007/s10238-021-00747-3

[15] Jiang Z, Li Y. CD93-targeted resveratrol-loaded PLGA nanoparticles remodel CD8+ T cell metabolism through AIF-mediated oxidative phosphorylation to overcome lung cancer immunotherapy resistance. Journal of Nanobiotechnology. 2026; 24: 382. https://doi.org/10.1186/s12951-026-04216-5

[16] Wang G, Yuan Y, Tang Y, Ma Q, Jiang H. Resveratrol inhibits pancreatic cancer progression via the ING5 signaling pathway. Scientific Reports. 2026; 16: 13473. https://doi.org/10.1038/s41598-026-44216-x

[17] Zhang L, Zeng Q, Kang Z, Fang S, Huang T, Pohla H, et al. Investigation of the impact of resveratrol on sublethal-dose ALA-PDT in glioblastoma cells. Photochemical & Photobiological Sciences : Official Journal of the European Photochemistry Association and the European Society for Photobiology. 2026; 25: 697–709. https://doi.org/10.1007/s43630-026-00877-1

[18] Hedayati N, Safari MH, Milasi YE, Kahkesh S, Farahani N, Khoshnazar SM, et al. Modulation of the PI3K/Akt signaling pathway by resveratrol in cancer: molecular mechanisms and therapeutic opportunity. Discover Oncology. 2025; 16: 669. https://doi.org/10.1007/s12672-025-02471-w

[19] Zhang M, Yuan W, Li C, Chen C, Liu X, Ma Z, et al. Resveratrol and N-acetylcystein reduce hepatic steatosis but enhance initiation and progression of hepatocellular carcinoma by inhibiting GST-pi-MAPK axis in mice. Frontiers in Pharmacology. 2025; 16: 1574039. https://doi.org/10.3389/fphar.2025.1574039

[20] Zhang Q, Tang X, Lu QY, Zhang ZF, Brown J, Le AD. Resveratrol inhibits hypoxia-induced accumulation of hypoxia-inducible factor-1alpha and VEGF expression in human tongue squamous cell carcinoma and hepatoma cells. Molecular Cancer Therapeutics. 2005; 4: 1465–1474. https://doi.org/10.1158/1535-7163.MCT-05-0198

[21] Liu Z, Peng Q, Li Y, Gao Y. Resveratrol enhances cisplatin-induced apoptosis in human hepatoma cells via glutamine metabolism inhibition. BMB Reports. 2018; 51: 474–479. https://doi.org/10.5483/BMBRep.2018.51.9.114

[22] Lin J, Schyschka L, Mühl-Benninghaus R, Neumann J, Hao L, Nussler N, et al. Comparative analysis of phase I and II enzyme activities in 5 hepatic cell lines identifies Huh-7 and HCC-T cells with the highest potential to study drug metabolism. Archives of Toxicology. 2012; 86: 87–95. https://doi.org/10.1007/s00204-011-0733-y

[23] Zhou Q, Li Y, Li X, Zhang S, Wang Y, Li Z, et al. Pleckstrin-2 promotes the progression of colorectal cancer via YTHDF2-mediated TYMS mRNA stability. Cellular and Molecular Life Sciences : CMLS. 2025; 82: 284. https://doi.org/10.1007/s00018-025-05782-x

[24] Ligabue A, Marverti G, Liebl U, Myllykallio H. Transcriptional activation and cell cycle block are the keys for 5-fluorouracil induced up-regulation of human thymidylate synthase expression. PloS One. 2012; 7: e47318. https://doi.org/10.1371/journal.pone.0047318

[25] Yang A, Wu Q, Chen Q, Yang J, Li H, Tao Y, et al. Cinobufagin restrains the growth and triggers DNA damage of human hepatocellular carcinoma cells via proteasome-dependent degradation of thymidylate synthase. Chemico-biological Interactions. 2022; 360: 109938. https://doi.org/10.1016/j.cbi.2022.109938

[26] Guo A, Chang Y, Lin J, Guo J, He Y, Wang C, et al. Resveratrol Enhances Anticancer Effects of Silybin on HepG2 Cells and H22 Tumor-bearing Mice via Inducing G2/M Phase Arrest and Increasing Bax/Bcl-2 Ratio. Combinatorial Chemistry & High Throughput Screening. 2025; 28: 89–98. https://doi.org/10.2174/0113862073263408231101105647

[27] Wang L, Shi C, Yu J, Xu Y. FOXM1-induced TYMS upregulation promotes the progression of hepatocellular carcinoma. Cancer Cell International. 2022; 22: 47. https://doi.org/10.1186/s12935-021-02372-2

[28] Zhou W, Xiao Y, Jiang Y, Zou A, Ruan J, Feng X, et al. Association of MTHFR rs9651118 and TYMS rs2790 Polymorphisms with Risk of Cancers: A Case-Control Study and Meta-analysis. Biochemical Genetics. 2025; 63: 4037–4056. https://doi.org/10.1007/s10528-024-10929-9

[29] Wilson PM, Danenberg PV, Johnston PG, Lenz HJ, Ladner RD. Standing the test of time: targeting thymidylate biosynthesis in cancer therapy. Nat Rev Clin Oncol. 2014;11:282–298. https://doi.org/10.1038/nrclinonc.2014.51

[30] Wu Q, Chen Q, Yang J, Zhang J, Yang A. Material basis revelation of anti-hepatoma effect of Huachansu (Cinobufacini) through down-regulation of thymidylate synthase. Chinese Herbal Medicines. 2024; 17: 127–138. https://doi.org/10.1016/j.chmed.2024.04.002

[31] Chen A, Yin K, Cui Q, Liu Y, Wan X, Yang W. Preventing liver carcinogenesis through the use of inhibitors targeting metabolic enzymes ACLY, G6PD, and TYMS, combined with 9-cis retinoic acid. International Journal of Biological Macromolecules. 2025; 331: 148378. https://doi.org/10.1016/j.ijbiomac.2025.148378

[32] Karim A, Khan HA, Ahmad F, Qaisar R. Improvement in postural imbalance with intake of resveratrol (polyphenolic phytoalexin) in patients of knee osteoarthritis. Explore (New York, N.Y.). 2026; 22: 103341. https://doi.org/10.1016/j.explore.2026.103341

[33] Karim A, Khan HA, Ahmad F, Qaisar R. Resveratrol supplementation improves functional performance in knee osteoarthritis by upregulating sirtuin 1: a randomized study. Inflammopharmacology. 2025; 33: 6877–6886. https://doi.org/10.1007/s10787-025-01967-9